

Sulfinamide Formation from the Reaction of Bacillithiol and Nitroxyl

Alberto Negrellos, Allison M. Rice, Patricia C. Dos Santos,* and S. Bruce King*


 Cite This: <https://doi.org/10.1021/acschembio.3c00526>


Read Online

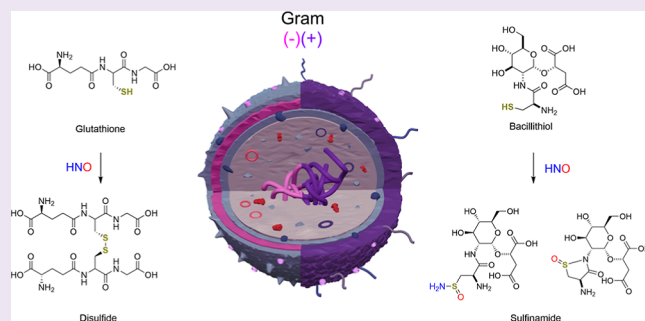
ACCESS |

Metrics & More

Article Recommendations

Supporting Information

ABSTRACT: Bacillithiol (BSH) replaces glutathione (GSH) as the most prominent low-molecular-weight thiol in many low G + C gram-positive bacteria. BSH plays roles in metal binding, protein/enzyme regulation, detoxification, redox buffering, and bacterial virulence. Given the small amounts of BSH isolated from natural sources and relatively lengthy chemical syntheses, the reactions of BSH with pertinent reactive oxygen, nitrogen, and sulfur species remain largely unexplored. We prepared BSH and exposed it to nitroxyl (HNO), a reactive nitrogen species that influences bacterial sulfur metabolism. The profile of this reaction was distinct from HNO oxidation of GSH, which yielded mixtures of disulfide and sulfinamide. The reaction of BSH and HNO (generated from Angeli's salt) gives only sulfinamide products, including a newly proposed cyclic sulfinamide. Treatment of a glucosamine–cysteine conjugate, which lacks the malic acid group, with HNO forms disulfide, implicating the malic acid group in sulfinamide formation. This finding supports a mechanism involving the formation of an N-hydroxysulfenamide intermediate that dehydrates to a sulfenium ion that can be trapped by water or internally trapped by an amide nitrogen to give the cyclic sulfinamide. The biological relevance of BSH reactivity toward HNO is provided through *in vivo* experiments demonstrating that *Bacillus subtilis* exposed to HNO shows a growth phenotype, and a strain unable to produce BSH shows hypersensitivity toward HNO in minimal medium cultures. Thiol analysis of HNO-exposed cultures shows an overall decrease in reduced BSH levels, which is not accompanied by increased levels of BSSB, supporting a model involving the formation of an oxidized sulfinamide derivative, identified *in vivo* by high-pressure liquid chromatography/mass spectrometry. Collectively, these findings reveal the unique chemistry and biology of HNO with BSH in bacteria that produce this biothiol.



Low-molecular-weight (LMW) thiols perform several critical roles in biological systems.¹ The reversible redox properties of LMW thiol/disulfide couples (thiol = reductant; disulfide = oxidant; Scheme 1) mediate the maintenance of a normal cellular redox status.¹ These redox functions are associated with the direct reactions of reactive oxygen, nitrogen, and sulfur species (ROS/RNS/RSS) with LMW thiols, translating redox chemistry into biology (Scheme 1).^{2–4} Thiols react with hydrogen peroxide (H_2O_2) to form sulfenic acids, reactive intermediates that promote ROS-based signaling.⁵ Hydrogen sulfide (H_2S) reacts with disulfides to give equilibrium mixtures of persulfides (RSSH),⁶ reactive species involved in bacterial sulfur mobilization (Scheme 1).^{7–9} Persulfides are more likely to form *in vivo* through H_2S condensation with activated thiols, such as sulfenic acids.⁶ Nitrosation of thiols yields S-nitrosothiols (RSNOs), which donate, transport, and store nitric oxide (NO, Scheme 1).¹⁰ These reactions have been described for glutathione (GSH), the predominant LMW thiol in higher organisms and most bacteria.^{11,12} In addition to its well-documented role in redox homeostasis, GSH also participates in detoxification pathways, metal binding, and protein/enzyme regulation.¹³ Several gram-positive bacterial species, however, do not produce GSH but instead produce

and utilize bacillithiol (BSH) or mycothiol (MSH), proposed surrogates of GSH in these organisms (Scheme 1).^{14,15}

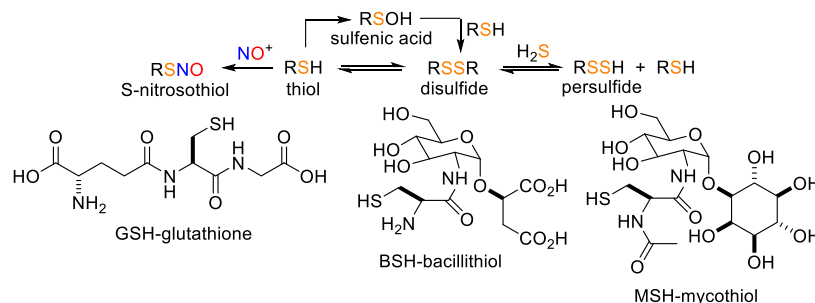
Discovered in 2009,¹⁶ BSH is the predominant LMW thiol found in low G + C gram-positive bacteria (*Firmicutes*), including *Bacillus*, *Staphylococcus*, *Streptococcus*, and *Deinococcus*. Structurally, BSH consists of an α -glycoside of L-malic acid and N-L-cysteinyl-D-glucosamine that forms both zinc and copper chelates.¹⁷ Its $pK_a = 7.97$, makes it more acidic than cysteine (Cys; $pK_a = 8.53$) or GSH ($pK_a = 8.93$).¹⁸ The redox potential of BSH/BSSB = -221 mV, a value closer to that of Cys (-223 mV) and higher than that of GSH (-240 mV).¹⁸ In *Bacillus subtilis*, the ratio of BSH/BSSB is $>100:1$ throughout different growth stages.¹⁸ BSH biosynthesis from N-acetyl glucosamine involves three enzymes: a glycosyltransferase (BshA), a deacetylase (BshB), and a ligase (BshC).^{19,20} Thus, inactivation of each of these biosynthetic genes results in

Received: August 25, 2023

Revised: November 14, 2023

Accepted: November 17, 2023

Scheme 1. Reversible Redox Properties of LMW Thiols and Structure of GSH, BSH, and MSH



the absence of BSH and leads to phenotypes similar but not identical to those associated with a lack of GSH in species producing this ubiquitous thiol.²¹

BSH participates in metal binding, mediation of responses to oxidative stress, and detoxification of xenobiotics.^{15,22} It influences metal homeostasis through zinc binding, iron-sulfur cluster assembly, and copper trafficking.¹⁵ Oxidative stress results in S-bacillithiolation of the only redox-sensitive cysteine residue in the organic hydroperoxide repressor (OhrR) in *B. subtilis*, leading to OhrA peroxiredoxin induction.¹⁵ Protein S-bacillithiolation appears as a widespread thiol-protection and redox-regulatory mechanism in *Firmicutes*.^{23,24} A bacillithiol S-transferase (BST, FosB) transfers BSH to fosfomycin, inactivating the antibiotic and providing a resistance mechanism.^{25,26} BSH detoxifies other electrophiles, including formaldehyde and methylglyoxal.¹⁵ Despite meaningful progress toward the characterization of BSH, the inventory of biological reactions involving this biothiol remains incomplete, especially the distinct reactivity of BSH compared to well-studied GSH and cysteine. Even less understood is the reactivity of BSH with RNS.

The direct and indirect reactivities of nitrogen oxides and LMW thiols have physiological significance and affect both the LMW and protein thiol redox equilibrium. In bacteria, NO modulates responses against oxygen- and nitrogen-reactive species (ROS/RNS).²⁷ In *B. subtilis* cultures, NO[•] triggers changes in the transcriptome associated with depression of Fur and PerR regulons.²⁸ Although the involvement of BSH is anticipated through pathways analogous to those described for Cys and GSH, mechanistic studies do not yet exist that characterize these reactions. Nonetheless, studies of H₂S homeostasis in *S. aureus* and *Enterococcus faecalis* show that, like H₂S, HNO increases BSSH and coenzyme A-SSH levels.^{29,30} This model suggests that the reaction of NO and H₂S yields HNO,³¹ which increases LMW persulfide formation.^{29,30} These persulfides, in turn, modify dithiol-containing repressors, such as CstR (CsoR-like sulfurtransferase repressor), which prevent transcription of the H₂S-oxidation systems that regulate sulfur trafficking.³² While the molecular mechanisms by which HNO increases persulfide formation and elicits physiological responses in bacteria remain unknown, these recent reports provide the premise for investigating the reactivity of BSH and HNO.

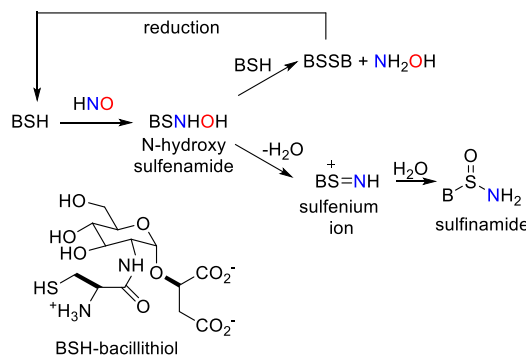
For the first time, we describe the products of the direct *in vitro* reaction of BSH with HNO and NO. *In vitro* studies here compare the reactivity of RNS to BSH to the reaction profile and products observed for GSH and Cys. The unexpectedly distinct reactivity of BSH with HNO, which predominantly modifies the thiol as a sulfonamide, reported in this work may be explained by the unique chemical structure of BSH and

suggests a role for the malic acid group. *In vitro* chemical analysis of synthetic BSH was complemented by *in vivo* experiments of *B. subtilis* cultures challenged with HNO. Analysis of LMW thiols in these cultures supports a model in which HNO leads to sulfonamide formation. Furthermore, the growth curve analysis shows that BSH-deficient strains of *B. subtilis* exhibit hypersensitivity to HNO, revealing the involvement of BSH in mediating responses against HNO stress. These findings form the basis for further investigation of the role of HNO in BSH-producing organisms, including those of biomedical relevance.

RESULTS AND DISCUSSION

Nitroxyl (azanone, HNO) is an emerging RNS related to NO through one-electron oxidation and proton loss that possesses unique chemistry/biology.^{33,34} HNO efficiently reacts as an electrophile with thiols to form an N-hydroxysulfenamide that condenses with excess thiol to yield a disulfide and hydroxylamine, or rearranges to produce a sulfonamide via dehydration to a sulfenium ion (Scheme 2).³³ The reaction of

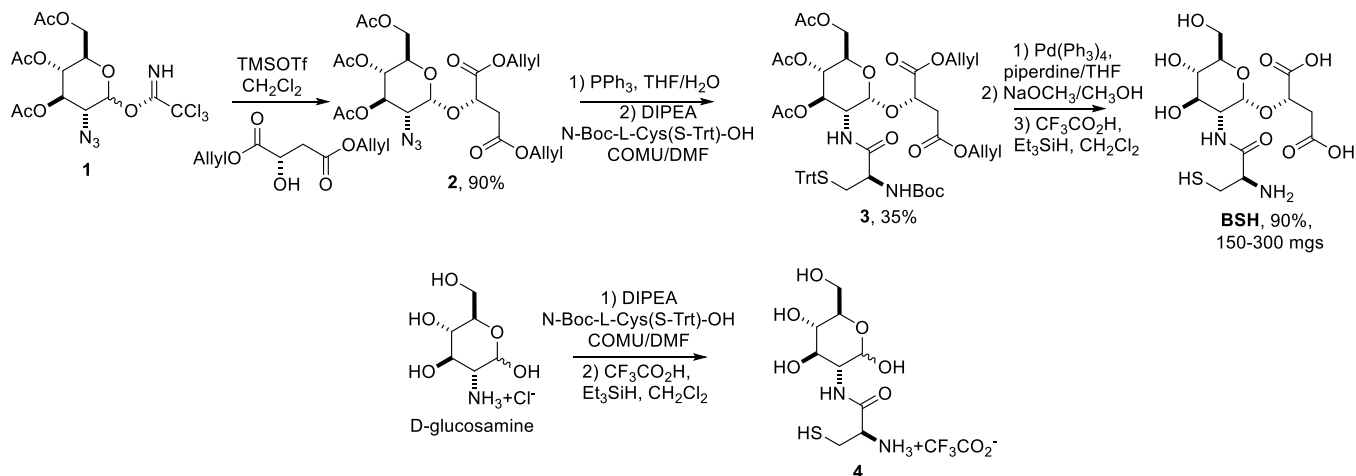
Scheme 2. Reactivity of Bacillithiol with Nitroxyl



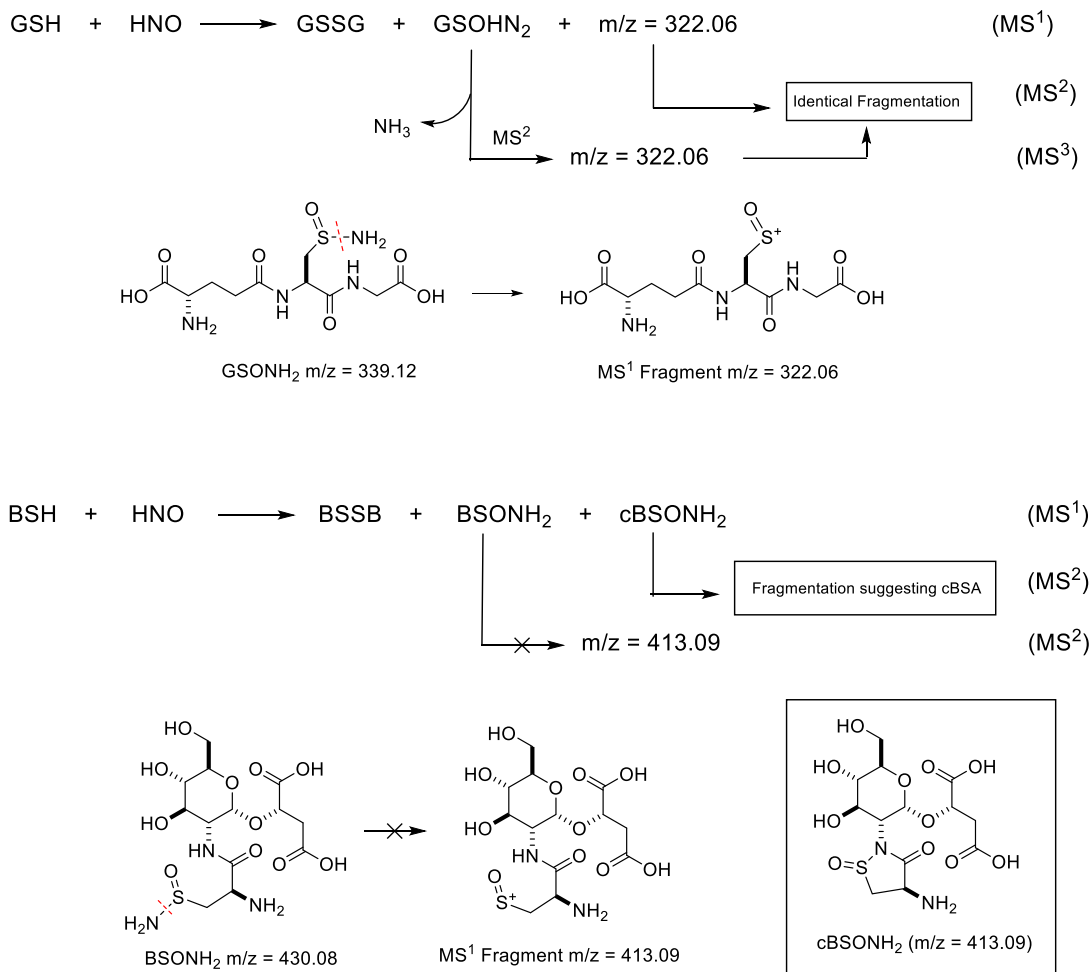
HNO with GSH produces a mixture of GSSG and the corresponding sulfonamide, with the ratio of sulfonamide/disulfide increasing at high [HNO] as predicted.^{35–37} The following experiments describe the reaction of BSH and HNO both *in vitro* and *in vivo* and reveal a product distribution different from that of the reaction of GSH and HNO.

Synthesis. Given the amount of BSH required to examine its reaction with HNO coupled with BSH's high commercial cost and difficulty in isolating from natural sources, BSH was synthesized using a combination of the two known BSH syntheses with some modifications (full details in *Supporting Information*).^{25,38} Coupling of the azido glucose-derived trichloroacetimidate (1) and diallyl malate with trimethylsilyl trifluoromethanesulfonate (TMSOTf) catalysis gave only α

Scheme 3. Synthesis of Bacillithiol and CysGlcN (4)



Scheme 4. Reaction Products of GSH and BSH with HNO



azide (2) in a 90% yield (Scheme 3).³⁸ In our hands, D-glucosamine provided a superior starting material for the preparation of large amounts of 1 (Scheme 3). Staudinger reduction followed by dimethylamino morpholino carbonium hexafluorophosphate (COMU)-based coupling of N-Boc L-cysteine (S-trityl) with 2 gave fully protected BSH (3) in a 35% yield (Scheme 3). Global deprotection of 3 yields BSH that demonstrates proton and carbon nuclear magnetic

resonance (NMR) spectra identical to those reported, providing material for the chemical investigation with HNO (Figures S1–S2).^{25,38}

Similarly, COMU-based coupling of N-Boc L-cysteine (S-trityl) with D-glucosamine hydrochloride followed by deprotection generates 2-(cysteinyl)amido-2-deoxy- α / β -D-glucopyranose (CysGlcN, 4, Figures S3–S5), a BSH derivative devoid of the malic acid group, to determine the effect the free

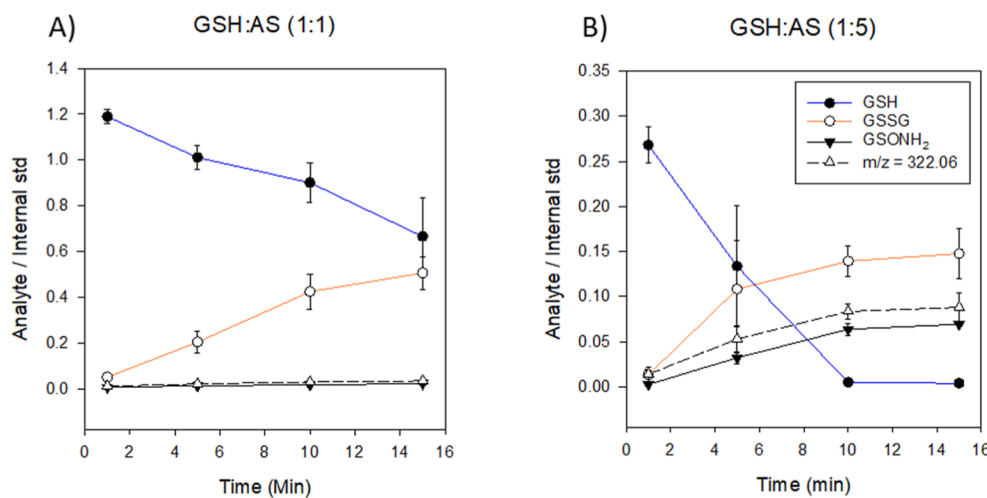


Figure 1. Reaction products of GSH with AS. Reaction progress ($n = 3$) of GSH with AS at 1:1 and 1:5 mol equiv. The reaction was analyzed in 5 min intervals starting from 1 min GSH $m/z = 308.15$ $[\text{M} + \text{H}]^+$ blue; GSSG $m/z = 613.16$ $[\text{M} + \text{H}]^+$ orange; GSONH₂ $m/z = 339.12$ $[\text{M} + \text{H}]^+$ black; and $m/z = 322.06$ $[\text{M} + \text{H}]^+$ dashed. (A) GSH 1 mM: AS 1 mM; (B) GSH 1 mM: AS 5 mM.

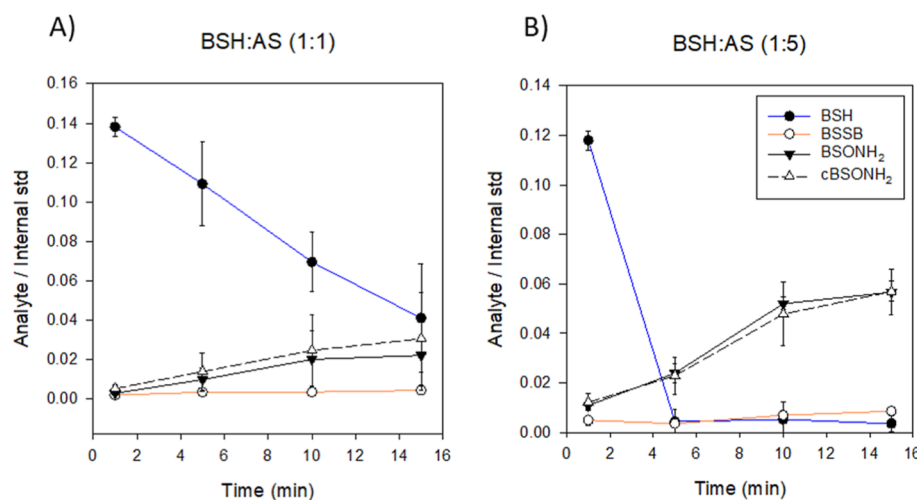


Figure 2. Reaction products of BSH with AS. Reaction progress ($n = 3$) of BSH with AS at 1:1 and 1:5 mol equiv. The reaction was analyzed in 5 min intervals starting from 1 min. BSH $m/z = 399.16$ $[\text{M} + \text{H}]^+$ blue; BSSB $m/z = 795.18$ $[\text{M} + \text{H}]^+$ orange; BSONH₂ $m/z = 430.12$ $[\text{M} + \text{H}]^+$ black; and cBSONH₂ $m/z = 413.07$ $[\text{M} + \text{H}]^+$ dashed.

carboxylic acid groups play in the reaction with HNO (Scheme 3).

In Vitro Reactions of BSH and GSH with HNO. Direct injection electrospray ionization mass spectrometry (ESI-MS) measurements of the reactions of GSH and BSH (1 mM) with the HNO donor Angeli's salt (AS, 1 or 5 mM) in HEPES buffer (10 mM, pH = 7.4) at RT (~ 20 °C) over 15 min were used to identify the reaction products. Figure S6 shows a product profile typical of the reaction of GSH and AS, consistent with the literature,^{35–37} giving GSSG as the major product over glutathione sulfonamide (GSONH₂, Scheme 4) even with excess HNO. Similar results were expected for the reaction of BSH and AS, but surprisingly, only negligible amounts of BSSB formed relative to bacillithiol sulfonamide (BSONH₂, Scheme 4, Figure S7). High-resolution mass spectrometry (HRMS) confirmed the chemical formulas of GSONH₂ and BSONH₂ (Figures S8 and S9). Quantitation by MS remains challenging in the absence of authentic sulfonamide standards; therefore, the ion count of interest was normalized to the ion count of the reaction buffer (Tris or

HEPES, $m/z = 122.13$ $[\text{M} + \text{H}]^+$, and $m/z = 238.98$ $[\text{M} + \text{H}]^+$, respectively), as the internal standard, with the ratio of the ion count of the analyte of interest to the internal standard being plotted against time.

Specifically, treatment of GSH (1 mM) with AS (1 mM) results in the decrease of thiol ($m/z = 308.05$ $[\text{M} + \text{H}]^+$) with the concomitant formation of disulfide ($m/z = 613.15$ $[\text{M} + \text{H}]^+$) at RT (~ 20 °C) for 15 min. At this concentration of AS, a significant portion of GSH remained unreacted after 15 min, consistent with the half-life of AS (16.8 min, pH = 7.36, 25 °C), and negligible amounts of GSONH₂ formed (Figure 1A, $m/z = 339.08$ $[\text{M} + \text{H}]^+$).^{39,40} Given the different ionizability of GSH, GSSG, or GSONH₂, ion counts do not necessarily reflect the absolute amounts of these species at a specific time but provide meaningful information about the relative amounts of each product over the course of the reaction. Increasing the concentration of AS to 5 mM produces GSSG as the major product with more significant levels of GSONH₂ (GSONH₂/GSSG = 1:2, Figure 1B), as expected. A closer examination of this mass spectrum revealed the formation of another peak at

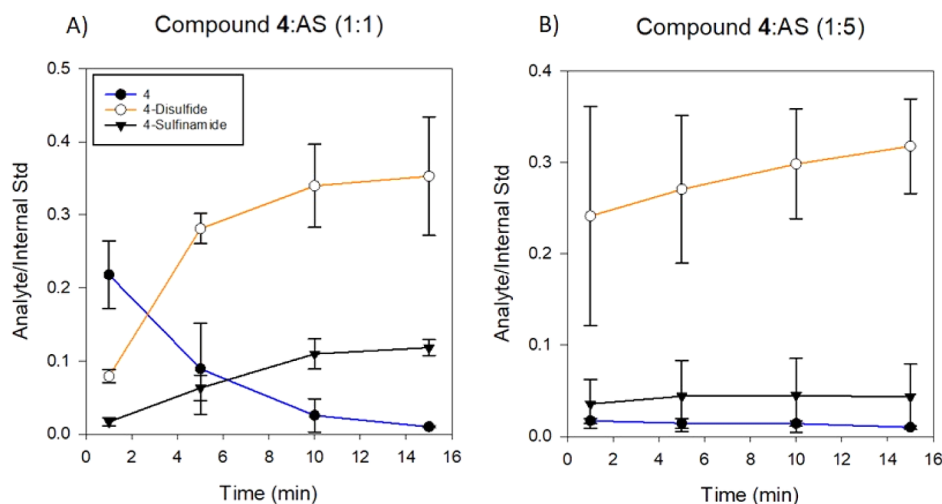


Figure 3. Reaction products of **4** with AS. Reaction progress ($n = 3$) of **4** with 1:1 and 1:5 mol equiv. Reaction was analyzed in 5 min intervals starting from 1 min. **4**, $m/z = 283.10$ [$M + H$]⁺ blue; **4**-disulfide, $m/z = 563.16$ [$M + H$]⁺ orange; and **4**-sulfonamide, $m/z = 314.10$ [$M + H$]⁺ gray. (A) **4** 1 mM: AS 1 mM; (B) **4** 1 mM: AS 5 mM.

$m/z = 322.06$ [$M + H$]⁺, suggesting ammonia loss from GSONH_2 . MS^2 analysis of GSONH_2 ($m/z = 339.08$ [$M + H$]⁺) resulted in $m/z = 322.06$ [$M + H$]⁺ as the major fragmentation product (Scheme 4 and Figure S10A–C). Further fragmentation of $m/z = 322.06$ (MS^3) resulted in a fragmentation fingerprint identical to the pattern observed in MS^1 for $m/z = 322.05$ (Figure S10D,E). This fragmentation pattern suggests that GSONH_2 ($m/z = 339.08$ [$M + H$]⁺) fragments in the mass spectrometer result in the observed $m/z = 322.06$ peak.

Similar analyses show the products of the reaction of BSH (1 mM) with AS (1 mM) over 15 min (Figure 2A). As expected, the amount of BSH ($m/z = 399.07$ [$M + H$]⁺) decreases, but unlike GSH, the reaction led to very little disulfide (BSSB, $m/z = 795.18$ [$M + H$]⁺) and formed products showing mass spectra that corresponded to BSH sulfonamide (BSONH_2 , Scheme 4, $m/z = 430.08$ [$M + H$]⁺, $\text{BSONH}_2/\text{BSSB} = 7:1$). Like GSH, this mass spectrum revealed the formation of a peak at $m/z = 413.07$ [$M + H$]⁺, suggesting loss of ammonia from BSONH_2 (Figure 2A). At low and high amplitudes (0.25–1.0), collision-induced dissociation (CID) MS^2 analysis of BSONH_2 ($m/z = 430.08$) did not produce a $m/z = 413.07$ peak as seen in MS^1 (Figure S11). Fragmentation of $m/z = 413.07$ generated fragments of $m/z = 278.93$ and 134.95, consistent with fragments derived from a cyclic sulfonamide (cBSONH_2 , Scheme 4). These results suggest that the observed $m/z = 413.07$ peak is indeed a reaction product of BSH and HNO and not a result of BSONH_2 fragmentation on the mass spectrometer. This newly described BSH modification finds precedence in the recently proposed cyclic sulfonamide generated by the treatment of BSH with HOCl.⁴¹ The reaction of BSH with excess AS (5 mM) gave similar results ($\text{BSONH}_2/\text{BSSB}$, 6:1, 15 min), with BSH being consumed after 5 min and the BSONH_2 to BSSB ratio not being greatly affected by the higher concentration of AS (Figure 2B). The use of the structurally and mechanistically distinct HNO donor, 2-bromo Piloyt's acid (2BPA, 1 and 5 mM), gives similar results, indicating the involvement of HNO regardless of the source (Figure S12).

Reactions of BSH with other oxidants or RNS identify sulfonamides as unique HNO-derived products. Treatment of

BSH (1 mM) with hydrogen peroxide (1 mM) generates BSSB (Figure S13).⁴¹ Exposure of BSH (1 mM) to sodium nitrite (5 mM, NO_2^-), the byproduct of AS salt decomposition and a potential nitrosating agent,⁴² does not yield $\text{BSONH}_2/\text{cBSONH}_2$ and only small amounts of BSSB (Figure S14). Reaction of BSH (1 mM) with (Z)-1-(*N,N*-diethylamino)-diazen-1-ium-1,2-diolate (5 mM, DEA/NO), a well-known NO donor,⁴³ generates BSSB over 15 min but does not form $\text{BSONH}_2/\text{cBSONH}_2$ (Figure S15). ESI-MS measurements show a small peak ($m/z = 428.11$) that may correspond to S-nitrosobacillithiol (BSNO), which could arise from the air oxidation of NO to a nitrosating species. These other common oxidants/RNS also fail to produce GSONH_2 from GSH, indicating a distinct chemical mechanism of the BSH and HNO reaction.

Mechanistic insight into how BSH structure regulates its unique reactivity toward HNO was probed by inspection of reaction products using structural fragments of BSH. First, L-Cys and *N*-acetyl cysteine (NAC, 1 mM) were reacted with AS and 2BPA (1 and 5 mM). As reported, the reaction of AS with L-Cys gave only cystine,⁴³ and NAC predominantly yields disulfide with a small amount of sulfonamide (Figures S16 and S17).⁴⁴ The currently accepted mechanism of sulfonamide formation involves acid-catalyzed *N*-hydroxysulfenium intermediate dehydration to the sulfenium ion (Scheme 2).³³ This mechanistic consideration, along with the ability of the malic acid group to influence solubility, act as a metal chelator, and impart enzymatic specificity (BshB), led us to hypothesize that the malic acid portion of BSH plays a critical role in directing sulfonamide formation in the BSH reaction with HNO. To test this hypothesis, we synthesized CysGlcN (**4**), which is the fragment of BSH lacking the malate group (Scheme 3). The reaction of synthetic CysGlcN (1 mM) with AS (1 and 5 mM) predominantly gave disulfide, little sulfonamide, and no apparent cyclic sulfonamide (Figure 3). This product distribution is strikingly distinct from that observed with BSH and is more similar to that of the reaction of HNO and GSH (Figures 1 and 2). As expected, the reaction of **4** with 2BPA gave similar results (Figure S18) that show the malic acid portion of the molecule facilitates $\text{BSONH}_2/\text{cBSONH}_2$ production.

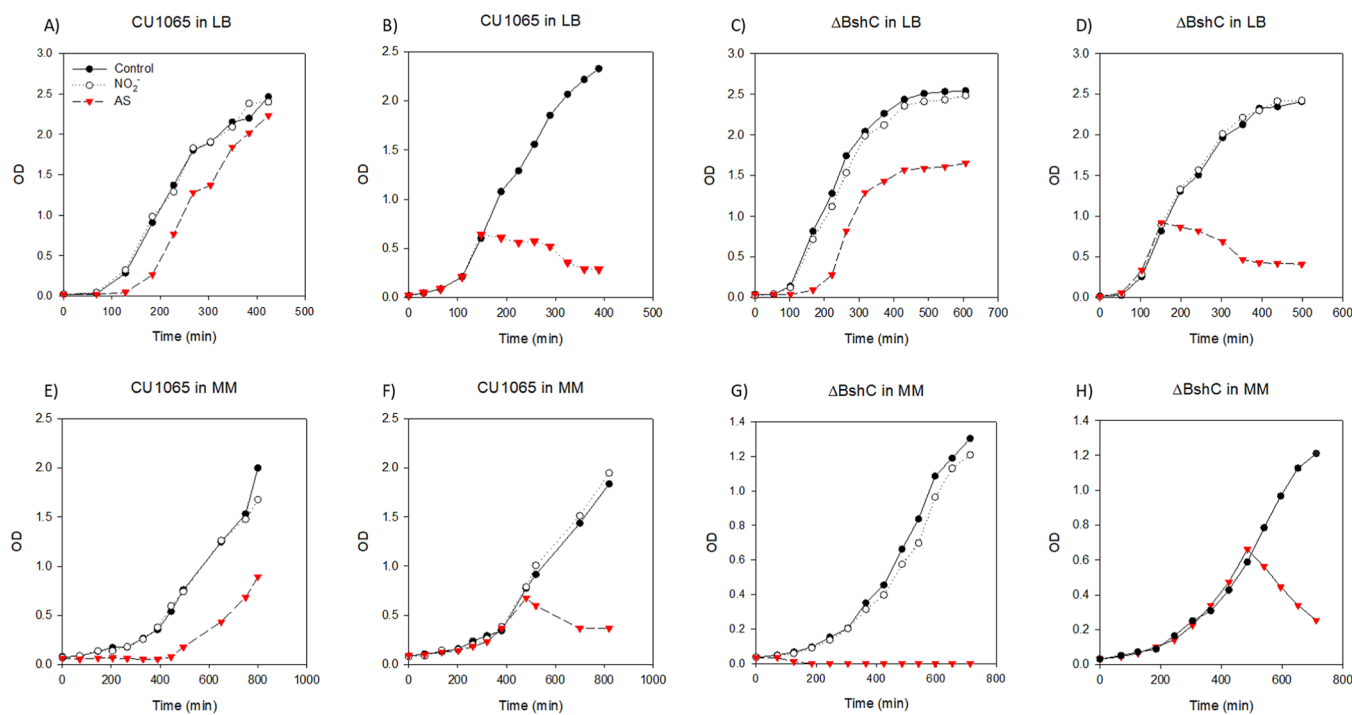


Figure 4. Effect of Angeli's salt on CU1065 and Δ BshC *B. subtilis* growth in LB and MM. Growth curves of *B. subtilis* CU1065 and Δ BshC cultures were challenged with Angeli salt (AS) at inoculation (~0.02 OD) or midlog (0.5–0.9 OD) in LB and Spizizen (MM) media: (A) WT in LB medium, NO_2^- (0.2 mM), and AS (0.2 mM); (B) WT in LB medium AS (0.2 mM); (C) Δ BshC in LB medium, NO_2^- (0.2 mM), and AS (0.2 mM); (D) Δ BshC in LB medium and AS (0.2 mM); (E) WT in MM, NO_2^- (0.2 mM), and AS (0.2 mM); (F) WT in MM AS (0.2 mM); (G) Δ BshC in MM medium, NO_2^- (0.2 mM), and AS (0.2 mM); and (H) Δ BshC in MM and AS (0.2 mM).

Given the ESI-MS evidence for sulfinamide formation and the lack of disulfide formation from the reaction of HNO and BSH, an overall decrease in free thiol and reducible modified thiols is expected and would provide further evidence of sulfinamide formation. Treatment of the BSH/AS reaction mixture with the thiol labeling reagent monobromobimane (mBBr) labeled free thiols in the mixture. Pretreatment of this reaction mixture with a reducing agent (DTT) converts reducible modified thiol derivatives back to free thiols that can be mBBr labeled. This procedure has successfully been used in our laboratories to determine ratios of BSH/BSSB in paraquat-stressed *B. subtilis* cells and should not detect the sulfinamide derivatives BSONH_2 or cBSONH_2 .²² Treatment of a reaction sample of BSH (1 mM) and AS (5 mM) followed by mBBr derivatization and high-performance liquid chromatography (HPLC) with fluorescence detection as compared to a synthetic BSH-mBBr adduct standard shows only 3.5% of the BSH remained or was converted to a DTT-reducible thiol derivative, supporting the accumulation of proposed reaction products BSONH_2 and cBSONH_2 (Scheme 4 and Figure 2). Similar experiments with GSH reveal that 18% remains as GSH or a reducible thiol derivative, consistent with the identification of GSSG by MS measurements (Figure 1). These results support the observed stability of sulfinamides under physiological conditions. Peptide-derived sulfinamides hydrolyze slowly but can be reduced to thiol over 26 h by DTT (50 mM DTT, 37 °C).³⁵ The reducing conditions used in this study (1.3 mM DTT, 50 °C, 10 min) are not expected to reduce the concentration of BSONH_2 / cBSONH_2 to BSH.

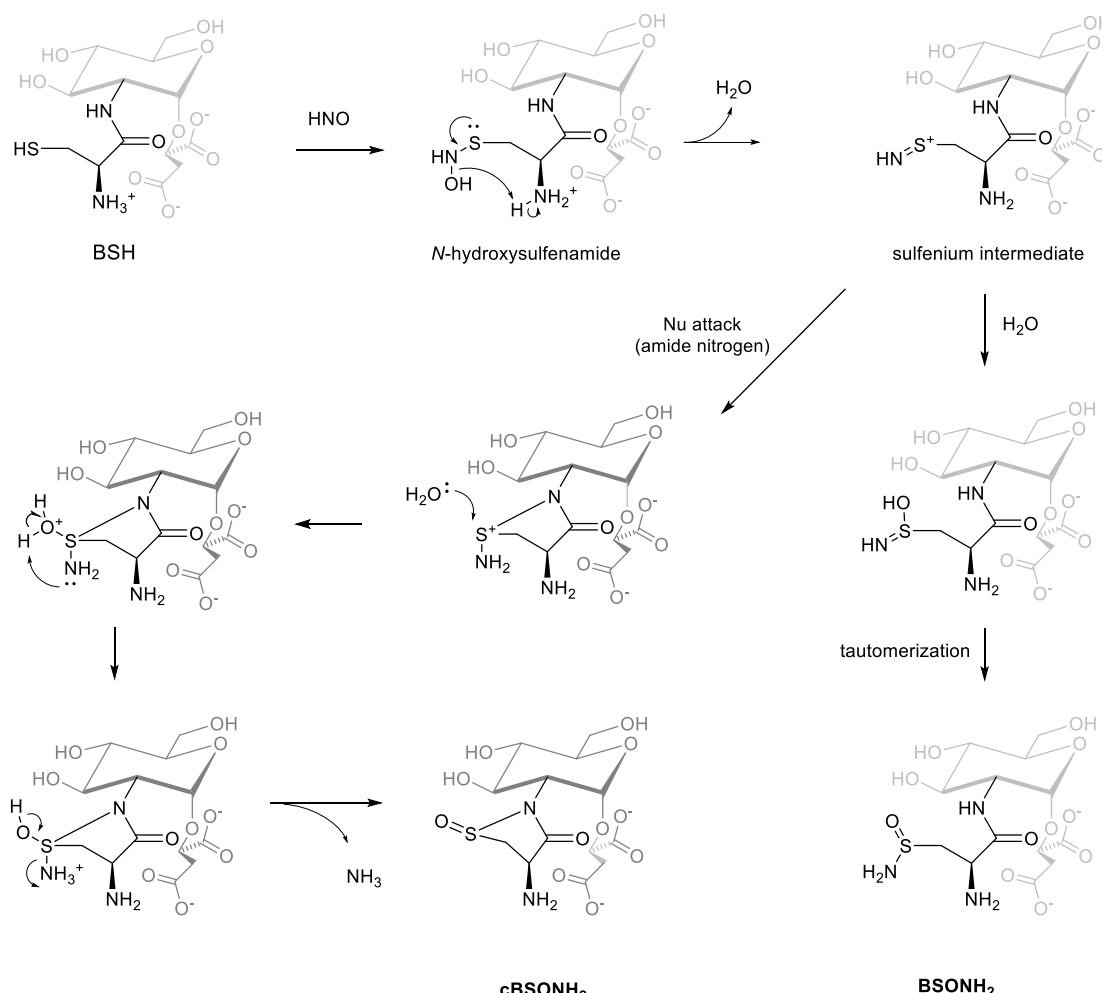
In Vivo Reactions of BSH with HNO. The in vitro reactions of BSH and HNO, particularly their formation of proposed structurally unique non-DTT-reducible sulfinamides

(BSONH_2 and cBSONH_2), prompted our consideration of the effects of HNO on BSH-producing bacteria and the in vivo reactivity of HNO with BSH. Therefore, the effect of HNO on *B. subtilis* cell viability was assessed in wild type (CU1065) and Δ bshC (HB110079), a strain that does not produce BSH. Both strains were grown in both rich (lysogeny broth) and minimal medium (Spizizen's minimal medium), with HNO being added at inoculation and midlog phase in separate cultures. Controls consisted of untreated bacteria and nitrite (NaNO_2)-treated bacterial growth.

The in vivo effects of the AS challenge were demonstrated for both *B. subtilis* wild-type and Δ bshC strains. A delay in the growth curve of *B. subtilis* wild-type grown in LB and MM was observed upon the addition of AS at the beginning of the growth (OD = 0.02), when compared to untreated and nitrite treated. Notably, the growth phenotype was more pronounced in MM cultures (Figure 4A,E). When AS was added during the midlog phase (OD = 0.6), a decrease in growth curve OD was observed for both LB and MM cultures, with MM having a more noticeable inhibition profile (Figure 4B,F). Remarkably, treatment of *B. subtilis* Δ bshC with AS at OD = 0.02 completely inhibited growth in MM and delayed growth in LB while seemingly reducing the stationary phase compared to the controls (Figure 4C,G). The addition of AS at OD = 0.5 for LB and MM growths resulted in a decrease in OD when compared with the wild-type experiments (Figure 4D,H). These results demonstrate an evident phenotypic sensitivity of *B. subtilis* lacking BSH to HNO exposure, indicating that BSH is an important biothiol in mediating HNO stress.

Given the results from growth experiments, the intracellular levels of BSH in reduced and oxidized forms were determined in *B. subtilis* wild-type cells before and after exposure to AS.

Scheme 5. Proposed Mechanism Promoting the Formation of Sulfurinamides from the Reaction of BSH and HNO



The levels of BSH in CU1065 cells cultured in minimal medium conditions were determined to be $2.20 \pm 0.13 \mu\text{mol/g}$ (dry weight), reflecting the amount of reduced BSH. Cell lysates pretreated with DTT captured BSH and modified thiols (BS-X, X = $-\text{H}$, $-\text{OH}$, $-\text{SH}$, $-\text{NO}$, $-\text{SProtein}$, $-\text{SB}$) and gave a total thiol concentration of $2.97 \pm 0.15 \mu\text{mol/g}$ (dry weight) (Figure S19). These values were used to calculate a redox ratio of 0.74 (BSH/total thiol). The average concentration of BSH in CU1065 cells cultured in a minimal medium and AS-treated was determined to be $1.65 \pm 0.07 \mu\text{mol/g}$ (determined from cells collected 30 min after AS addition at $\text{OD} = 0.50\text{--}0.70$, $n = 3$). Analysis of total thiol from DTT treatment led to the detection of $2.0 \pm 0.20 \mu\text{mol/g}$ of BSH, representing a BSH/total thiol redox ratio of 0.82. The addition of HNO to *B. subtilis* results in a reduction in the total amount of BSH, with the BSH/total thiol redox ratio remaining similar to excess reduced BSH. The analysis of in vivo levels of BSH is compatible with results from in vitro reactions of BSH and AS, where the formation of a non-DTT reducible sulfenamide would decrease the overall amount of BSH observed but permit cellular processes to maintain a cellular redox ratio.

HPLC-HRMS of the LMW fraction of soluble extracts from wild type *B. subtilis* cultured in LB and challenged with 0.2 mM AS led to the detection of BSONH₂ (Figure S20). Internal addition of the in vitro reaction mixture of BSH and HNO confirms the identity of BSONH₂, exhibiting the same mass

and retention time (Figure S20). Similar LC-HRMS analysis of control samples not treated with AS fails to provide evidence for BSONH₂, which appears only upon addition of the in vitro reaction mixture (Figure S20). Growth in the presence of excess 2 mM AS showed BSONH₂ and cBSONH₂, cyclic sulfenamide formation (Figure S20). These analyses provide the first evidence for the in vivo reactivity of HNO with BSH in *B. subtilis*, leading to the formation of sulfenamide products. The reaction products of in vitro BSH and HNO chemistry were also observed within *B. subtilis* cells.

While the molecular mechanisms by which HNO increases persulfide formation and elicits physiological responses in bacteria remain unknown, a simple model of persulfide formation would involve H₂S trapping of the N-hydroxysulfenamide that forms from the addition of HNO to BSH (Schemes 2 and 5). Our initial expectation was that BSH would behave similarly to GSH and generate mixtures of BSSB and sulfenamide upon reaction with HNO, but ESI-MS experiments reveal only the formation of BSH sulfenamide (BSONH₂) and virtually no BSSB. Comparison experiments using GSH gave both GSSG and sulfenamide (GSONH₂).^{35,36,45–47} Close examination of these mass spectra indicates that BSH forms a second product with HRMS confirming NH₃ loss, and we propose that an internal nitrogen atom of an amide bond participates in forming the 5-membered ring cyclic sulfenamide (cBSONH₂, Figure 2), and

Scheme 5). The lack of pure synthetic standards of BSONH_2 /c BSONH_2 , as well as GSONH_2 , limits our ability to monitor these reactions and assign chemical yields. Cyclic sulfenamides form in amide-containing thiols upon treatment with hydrogen peroxide, and a cyclic sulfonamide of BSH has recently been reported upon treatment of BSH with HOCl.^{41,48} These authors propose that this product arises from the conversion of the sulfinic acid to the sulfinyl chloride, followed by amide nitrogen condensation and further oxidation.⁴⁸ Treatment of serum albumin with HNO forms a cross-linked cyclic sulfonamide with a terminal amine group of lysine.⁴⁹ The addition of BSH to HNO gives the *N*-hydroxysulfenamide (BSNHOH, **Scheme 5**) and water loss from BSNHOH gives the sulfenium ion that reacts with water to yield BSONH_2 , following the canonical reaction of thiols with HNO (**Scheme 5**). Being electrophilic, the sulfenium ion can undergo intramolecular cyclization to c BSONH_2 (**Scheme 5**) and suggests potential targets for directed nucleophilic trapping strategies. The lack of BSSB formation indicates that BSNHOH loses water faster to yield sulfenamides compared to its GSH-derived counterpart, which forms significant amounts of GSSG. Such results argue against the formation of BSSH from the reaction of BSNHOH and H_2S .

Since the reaction of HNO with BSH led to a distinct product composition when compared to equivalent reactions with GSH, we investigated the chemical and structural features of BSH contributing to this novel reaction profile. The L-malate portion of BSH potentially facilitates water loss from the BSH *N*-hydroxysulfenamide intermediate that results in ultimate sulfenamide products. In this proposed reaction scheme, the malic acid carboxylic groups donate a proton to the cysteinyl amine to assist in water loss from the *N*-hydroxysulfenamide intermediate to the sulfenium ion. Thus, the malate carboxylate groups, the cysteinyl amine, and the thiol represent a “catalytic triad” type system that facilitates a proton shuttle. The malate carboxylate groups would also provide stabilization of the charged amine ($-\text{NH}_3^+$) that conceivably permits an easier proton transfer to BSNHOH. The addition of water or the amide nitrogen atom to the sulfenium ion generates BSONH_2 or c BSONH_2 , respectively (**Scheme 5**). The molecular arrangement (a *cis* relationship of the cysteine and malic acid groups) likely facilitates proton transfer at a rate faster than that of GSH and differentiates the observed products. In c BSONH_2 formation, the amide nitrogen proton may participate in a hydrogen bond with a malate carboxylate, increasing its ability to act as a nucleophile while simultaneously supporting proton transfer from the cysteinyl amine group. Thus, we propose that the malic acid group of bacillithiol acts as an acid catalyst for the formation of the sulfenium ion intermediate that directs the route for sulfenamide formation and not disulfide (**Scheme 5**). The reaction profile of GlcNCys (4) supports this proposed mechanism, in which the reaction with AS predominantly yields BSSB (**Figure 3**). Likewise, the reaction of HNO with Cys only gives disulfide and the reaction of HNO with NAC mainly forms disulfide, further indicating that the availability of an acid proton influences product outcome.^{44,49} More structurally specific substrates and a variety of reaction conditions, in addition to authentic sulfenamide standards, are needed to determine the factors that control the ratio of disulfide to sulfenamide in these reactions. Importantly, the reaction of HNO and BSH generates only sulfenamides

(BSONH_2 /c BSONH_2) under the conditions examined in this work.

The exclusive formation of BSONH_2 and c BSONH_2 *in vitro* obviously led to the question of whether these products form *in vivo*. Growth curve analysis shows that cells that cannot produce BSH show a sensitivity to HNO (**Figure 4**). *B. subtilis* cells treated with AS show an overall decrease in the amount of BSH while maintaining a similar BSH/BSSB ratio (**Figure S19**). These results, coupled with the *in vitro* observation of exclusive sulfenamide formation and the general chemical resistance of sulfenamides to reduction, suggest the formation of an oxidized thiol derivative.^{35,45} Further LC-HRMS experiments reveal the presence of an adduct of mass equivalent to the mass of BSONH_2 only in *B. subtilis* cells treated with AS. Ongoing work is aimed at generating authentic standards and a sensitive method to quantify these byproducts in complex mixtures such as cell extracts and live cells. Nevertheless, the findings presented in this study support a simplified model to explain these observations, including the reaction of HNO with BSH to yield sulfenamide while the remaining BSH maintains a similar redox balance of BSH/BSSB that ultimately affords protection against this reactive nitrogen species. Numerous questions remain, including whether biological systems can recycle sulfenamides into BSH, what are the ultimate cellular targets of HNO, and whether HNO has antibiotic potential.

In summary, the *in vitro* and *in vivo* reactions of BSH with HNO give sulfenamide (BSONH_2 /c BSONH_2) products and not disulfide (BSSB), in contrast to the reaction of GSH and HNO. This reactivity appears to be related to the presence of the malate group that may alter the reaction pathway by facilitating the formation of the reactive sulfenium ion. Cells incapable of producing BSH demonstrate a phenotypic sensitivity to HNO, and treating the wild-type *B. subtilis* with HNO leads to decreased levels of BSH, consistent with possible *in vivo* sulfenamide formation. This work highlights sulfenamides as nonreducible modified thiol derivatives in redox biochemistry and begins to define the reactivity of HNO in these bacteria, which contain a bacterial NO synthase.⁵⁰ The reduction of NO to HNO with H_2S and other potential H_2S -mediated 2-electron reductions of oxidized NO species (nitrite, nitrosonium ion, and S-nitrosothiols) potentially places HNO at the chemical intersection of NO/ H_2S signaling. These studies could impact our understanding of normal bacterial sulfur metabolism and form the basis for new antibiotic strategies.

METHODS

In Vitro Analysis. General Mass Spectrometry. Low-resolution MS measurements were made using an Amazon SL and Shimadzu autosampler. Samples were directly injected at a flow rate of 0.5 mL min^{-1} in 0.1% formic acid (FA)/50% acetonitrile with a resolution of 2000 in a continuous scan in positive mode. HRMS analysis was carried out by direct injection on an LTQ Orbitrap XL mass spectrometer (Thermo Fisher Scientific). Reactions were directly injected at a flow rate of $10 \mu\text{L min}^{-1}$ in 0.1% FA/50% acetonitrile. Scans used for analysis were performed in the ion trap, operating in full scan mode with a resolution of 2000 and continuous scan mode in positive mode.

Reactions of Thiols with Angeli's Salt and 2-Bromo Piloy's Acid. Freshly prepared 1 mM solutions of thiols in 4-(2-hydroxyethyl)-1-piperazine ethanesulfonic acid (HEPES) buffer (25 mM, pH = 7.4) were incubated with equimolar and 5-fold molar excesses of AS (added as a solid). The reaction products were analyzed over time in

positive mode ESI-MS at 1, 5, 10, and 15 min. All samples were analyzed in triplicate. A second set of thiol solutions (1.2 mM) was incubated with 2BPA (0.2 mL, 5 mM in DMSO for equimolar; 0.2 mL, 25 mM in DMSO for 5-fold excess), and the reaction products were analyzed over time by positive mode ESI-MS at 1, 5, 10, and 15 min. All samples were analyzed in triplicate. A sample of BSH and GSH treated with AS (1:5) was used for HRMS analysis.

In Vivo Analysis. Bacterial Strains and Culture Conditions. Bacterial strains of *B. subtilis* CU1065 and HB110079 ($\Delta bshC$) were kindly provided by Helmann.⁵¹ Preinocula of these strains were prepared from a single colony of a day-old plate in 5 mL of lysogeny broth (LB) medium. Starter cultures were used to prepare a 125 mL preinoculum (LB medium incubated at 37 °C and 170 rpm) that was used to grow 500 mL cultures in LB or Spizizen's minimal medium (MM). Preinoculum cells used for MM growths were washed in PBS before incubation and collected by centrifugation. All growths were incubated at 37 °C under shaking conditions, and the optical densities at 600 nm were recorded before and after treatment with NaNO₂ and AS.

Angel's Salt and Nitrite Challenge to *B. subtilis* Cultures. The effects of HNO stress were determined through treatment at the beginning (lag) and later (log) stages of *B. subtilis* liquid culture growth. In one series of experiments, 0.2 mM AS or 0.2–1 mM NaNO₂ was added to a culture of *B. subtilis* CU1065 and HB110079 at an OD 0.02–0.06. Each culture was grown concurrently to OD = 1.2–2.5, while optical density was recorded in 30–50 min intervals. For exponential phase experiments, 0.2 mM AS or 0.2–1 mM NaNO₂ (final concentration) was added to individual cultures during midlog phase (OD 0.5–0.9) and grown concurrently for an additional 6 h. Optical readings were recorded throughout the length of the incubation in 30–50 min intervals. For biological thiol analysis (BSH), the CU1065 strain was grown in MM (500 mL) in a 37 °C shaker to OD = 0.5 before the addition of 0.2 mM AS. The cultures were incubated for an additional 30 min after AS treatment (as were untreated cultures), and cells were harvested by centrifugation and stored at –20 °C for no more than 24 h before analysis using a modified version of a previously described mBBr derivatization procedure.⁵²

Cellular Bacillithiol Analysis. The redox status of BSH in *B. subtilis* CU1065 was estimated for exponential-phase cells grown in a minimal medium. Cultures of *B. subtilis* (500 mL) were grown in LB medium as described previously and harvested at OD₆₀₀ = 0.51–0.57. The cell pellets from the 500 mL culture were frozen at –20 °C and used for analysis within 24 h. Each cell pellet was resuspended in 4 mL of 25 mM HEPES buffer, 5 mM diethylenetriamine pentaacetic acid (DTPA), pH 8, and split into 4 equal portions of 1 mL of cell suspension. For analysis of reduced thiols, one portion was extracted with 0.3 mL of prewarmed (60 °C) acetonitrile containing 3 mM mBBr and incubated at 60 °C for 15 min, cooled to RT, and acidified with 5 μ L of 5 M methanesulfonic acid. To determine the fluorescence background, the second portion was extracted with 0.3 mL of prewarmed (60 °C) acetonitrile containing 5 mM N-ethylmaleimide (NEM) and incubated at 60 °C for 15 min prior to incubation with mBBr as described above. For analysis of total thiol content, the third portion was combined with 0.1 mL of aqueous 1.3 mM DTT in 25 mM HEPES buffer, pH = 8, and 5 mM DTPA, and incubated at 50 °C for 10 min prior to incubation with mBBr, as described above. The three fractions were centrifuged for 5 min to remove cell debris, and the supernatant was diluted 10-fold in 0.01 N HCl for HPLC analysis. The last portion of resuspended cells was centrifuged for 5 min, the supernatant was removed, and the cell pellet was dried in a speed vacuum to obtain the dry weight. The redox ratio was expressed as thiol/disulfide or RSH/RSSR and it was determined for BSH and cysteine.

HPLC Methodology. HPLC of in vitro and in vivo analyses was carried out with a Waters 2475 multiluminescence detector and a Waters 2695 separation module. The fluorescence detector was set to λ_{ex} = 385 and λ_{em} = 460 nm for the excitation and emission wavelengths. Separation of analytes was carried out using an Agilent Poroshell column (EC-C18, 4 mm, 4.6 \times 250 mm) at 40 °C with a

flow rate of 0.5 mL/min. Mobile phase A was HPLC-grade methanol; mobile phase B was 0.1% acetate buffer (v/v, pH = 3.95) prepared with ASTM-Type 1 water (Table S1). Calibration curves (Figure S21) for BSH, GSH, and Cys were made from chemical standards, resulting in BSMB (16.6–17.3 min), GSmB (19.9–20.6 min), and CysMB (17.6–18.2 min). Standard thiols were derivatized with mBBr in acetonitrile in HEPES buffer (25 mM, pH 8, 5 mM DTPA) and incubated at 60 °C while protected from light. The derivatization was quenched with 5 μ L 5 M methanesulfonic acid and diluted in 0.01 N HCl to calibrate the curve concentrations.

ASSOCIATED CONTENT

Supporting Information

The Supporting Information is available free of charge at <https://pubs.acs.org/doi/10.1021/acschembio.3c00526>.

General BSH synthetic procedures and ¹H and ¹³C NMR spectra, mass spectrometry data for the reactions of HNO with GSH and BSH and control reactions, BSH and Cys quantitation data from *B. subtilis*, in vivo detection of BSONH₂ in AS-treated *B. subtilis*, and calibration curves for HPLC standards (PDF)

AUTHOR INFORMATION

Corresponding Authors

Patricia C. Dos Santos — Department of Chemistry, Wake Forest University, Winston-Salem, North Carolina 27107, United States;  orcid.org/0000-0002-3364-0931; Email: dossanpc@wfu.edu

S. Bruce King — Department of Chemistry, Wake Forest University, Winston-Salem, North Carolina 27107, United States;  orcid.org/0000-0002-8647-8026; Email: kingsb@wfu.edu

Authors

Alberto Negrellos — Department of Chemistry, Wake Forest University, Winston-Salem, North Carolina 27107, United States

Allison M. Rice — Department of Chemistry, Wake Forest University, Winston-Salem, North Carolina 27107, United States

Complete contact information is available at: <https://pubs.acs.org/10.1021/acschembio.3c00526>

Funding

Financial support for this work was provided by the National Science Foundation (NSF MCB-176536, Dos Santos), the National Institutes of Health (R15GM151698, King), and Wake Forest University.

Notes

The authors declare no competing financial interest.

ACKNOWLEDGMENTS

Financial support for this work was provided by the National Science Foundation (NSF MCB-176536, Dos Santos), the National Institutes of Health (R15GM151698, King), and Wake Forest University.

REFERENCES

- Wang, M.; Zhao, Q.; Liu, W. The Versatile Low-Molecular-Weight Thiols: Beyond Cell Protection. *BioEssays* 2015, 37 (12), 1262–1267.
- Gruhlke, M. C. H.; Slusarenko, A. J. The Biology of Reactive Sulfur Species (RSS). *Plant Physiol. Biochem.* 2012, 59, 98–107.

(3) Sies, H.; Jones, D. P. Reactive Oxygen Species (ROS) as Pleiotropic Physiological Signalling Agents. *Nat. Rev. Mol. Cell Biol.* **2020**, *21* (7), 363–383.

(4) Patel, R. P.; McAndrew, J.; Sellak, H.; White, C. R.; Jo, H.; Freeman, B. A.; Darley-Usmar, V. M. Biological Aspects of Reactive Nitrogen Species. *Biochim. Biophys. Acta, Bioenerg.* **1999**, *1411* (2–3), 385–400.

(5) Gupta, V.; Carroll, K. S. Sulfinic Acid Chemistry, Detection and Cellular Lifetime. *Biochim. Biophys. Acta. Gen. Subj.* **2014**, *1840* (2), 847–875.

(6) Cuevasanta, E.; Lange, M.; Bonanata, J.; Coitíño, E. L.; Ferrer-Sueta, G.; Filipovic, M. R.; Alvarez, B. Reaction of Hydrogen Sulfide with Disulfide and Sulfinic Acid to Form the Strongly Nucleophilic Persulfide. *J. Biol. Chem.* **2015**, *290* (45), 26866–26880.

(7) Kabil, O.; Banerjee, R. Redox Biochemistry of Hydrogen Sulfide. *J. Biol. Chem.* **2010**, *285* (29), 21903–21907.

(8) Ida, T.; Sawa, T.; Ihara, H.; Tsuchiya, Y.; Watanabe, Y.; Kumagai, Y.; Suematsu, M.; Motohashi, H.; Fujii, S.; Matsunaga, T.; Yamamoto, M.; Ono, K.; Devarie-Baez, N. O.; Xian, M.; Fukuto, J. M.; Akaike, T. Reactive Cysteine Persulfides and S-Polythiolation Regulate Oxidative Stress and Redox Signaling. *Proc. Natl. Acad. Sci. U.S.A.* **2014**, *111*, 7606–7611.

(9) Millikin, R.; Bianco, C. L.; White, C.; Saund, S. S.; Henriquez, S.; Sosa, V.; Akaike, T.; Kumagai, Y.; Soeda, S.; Toscano, J. P.; Lin, J.; Fukuto, J. M. The Chemical Biology of Protein Hydopersulfides: Studies of a Possible Protective Function of Biological Hydopersulfide Generation. *Free Radical Biol. Med.* **2016**, *97*, 136–147.

(10) Williams, D. L. H. The Chemistry of S-Nitrosothiols. *Acc. Chem. Res.* **1999**, *32* (10), 869–876.

(11) Ku, J. W. K.; Gan, Y.-H. New Roles for Glutathione: Modulators of Bacterial Virulence and Pathogenesis. *Redox Biol.* **2021**, *44*, 102012.

(12) Moldogazieva, N. T.; Mokhosoev, I. M.; Feldman, N. B.; Lutsenko, S. V. ROS and RNS Signalling: Adaptive Redox Switches through Oxidative/Nitrosative Protein Modifications. *Free Radic. Res.* **2018**, *52* (5), 507–543.

(13) Forman, H. J.; Zhang, H.; Rinna, A. Glutathione: Overview of Its Protective Roles, Measurement, and Biosynthesis. *Mol. Aspects Med.* **2009**, *30* (1–2), 1–12.

(14) Reyes, A. M.; Pedre, B.; De Armas, M. I.; Tossounian, M.-A.; Radi, R.; Messens, J.; Trujillo, M. Chemistry and Redox Biology of Mycothiol. *Antioxid. Redox Signaling* **2018**, *28* (6), 487–504.

(15) Chandrangs, P.; Loi, V. V.; Antelmann, H.; Helmann, J. D. The Role of Bacillithiol in Gram-Positive Firmicutes. *Antioxid. Redox Signaling* **2018**, *28* (6), 445–462.

(16) Newton, G. L.; Rawat, M.; La Clair, J. J.; Jothivasan, V. K.; Budiarto, T.; Hamilton, C. J.; Claiborne, A.; Helmann, J. D.; Fahey, R. C. Bacillithiol Is an Antioxidant Thiol Produced in Bacilli. *Nat. Chem. Biol.* **2009**, *5* (9), 625–627.

(17) Ma, Z.; Chandrangs, P.; Helmann, T. C.; Romsang, A.; Gaballa, A.; Helmann, J. D. Bacillithiol is a major buffer of the labile zinc pool in *Bacillus subtilis*. *Mol. Microbiol.* **2014**, *94* (4), 756–770.

(18) Sharma, S. V.; Arbach, M.; Roberts, A. A.; Macdonald, C. J.; Groom, M.; Hamilton, C. J. Biophysical Features of Bacillithiol, the Glutathione Surrogate of *Bacillus subtilis* and Other Firmicutes. *ChemBioChem* **2013**, *14* (16), 2160–2168.

(19) Cross-functionalities of *Bacillus* deacetylases involved in bacillithiol biosynthesis and bacillithiol-S-conjugate detoxification pathways, *Biochemical Journal*; Portland Press. <https://portlandpress.com/biochemj/article/454/2/239/46504/Cross-functionalities-of-Bacillus-deacetylases> (accessed 2023-02-20).

(20) Parsonage, D.; Newton, G. L.; Holder, R. C.; Wallace, B. D.; Paige, C.; Hamilton, C. J.; Dos Santos, P. C.; Redinbo, M. R.; Reid, S. D.; Claiborne, A. Characterization of the N-Acetyl- α -d-glucosaminyl l-Malate Synthase and Deacetylase Functions for Bacillithiol Biosynthesis in *Bacillus anthracis*. *Biochemistry* **2010**, *49* (38), 8398–8414.

(21) Posada, A. C.; Kolar, S. L.; Dusi, R. G.; Francois, P.; Roberts, A. A.; Hamilton, C. J.; Liu, G. Y.; Cheung, A. Importance of Bacillithiol in the Oxidative Stress Response of *Staphylococcus aureus*. *Infect. Immun.* **2014**, *82* (1), 316–332.

(22) Fang, Z.; Dos Santos, P. C. Protective Role of Bacillithiol in Superoxide Stress and Fe-S Metabolism in *Bacillus subtilis*. *MicrobiologyOpen* **2015**, *4* (4), 616–631.

(23) Chi, B. K.; Roberts, A. A.; Huyen, T. T. T.; Bäsel, K.; Becher, D.; Albrecht, D.; Hamilton, C. J.; Antelmann, H. S-Bacillithiolation Protects Conserved and Essential Proteins Against Hypochlorite Stress in Firmicutes Bacteria. *Antioxid. Redox Signaling* **2013**, *18* (11), 1273–1295.

(24) Imber, M.; Huyen, N. T. T.; Pietrzyk-Brzezinska, A. J.; Loi, V. V.; Hillion, M.; Bernhardt, J.; Thärichen, L.; Kolšek, K.; Saleh, M.; Hamilton, C. J.; Adrian, L.; Gräter, F.; Wahl, M. C.; Antelmann, H. Protein S-Bacillithiolation Functions in Thiol Protection and Redox Regulation of the Glyceraldehyde-3-Phosphate Dehydrogenase Gap in *Staphylococcus aureus* Under Hypochlorite Stress. *Antioxid. Redox Signaling* **2018**, *28* (6), 410–430.

(25) Lamers, A. P.; Keithly, M. E.; Kim, K.; Cook, P. D.; Stec, D. F.; Hines, K. M.; Sulikowski, G. A.; Armstrong, R. N. Synthesis of Bacillithiol and the Catalytic Selectivity of FosB-Type Fosfomycin Resistance Proteins. *Org. Lett.* **2012**, *14* (20), 5207–5209.

(26) Roberts, A. A.; Sharma, S. V.; Strankman, A. W.; Duran, S. R.; Rawat, M.; Hamilton, C. J. Mechanistic Studies of FosB: A Divalent-Metal-Dependent Bacillithiol-S-Transferase That Mediates Fosfomycin Resistance in *Staphylococcus aureus*. *Biochem. J.* **2013**, *451* (1), 69–79.

(27) Chautrand, T.; Souak, D.; Chevalier, S.; Duclairoir-Poc, C. Gram-Negative Bacterial Envelope Homeostasis under Oxidative and Nitrosative Stress. *Microorganisms* **2022**, *10* (5), 924.

(28) Fuangthong, M.; Herbig, A. F.; Bsat, N.; Helmann, J. D. Regulation of the *Bacillus subtilis* Fur and PerR Genes by PerR: Not All Members of the PerR Regulon Are Peroxide Inducible. *J. Bacteriol.* **2002**, *184* (12), 3276–3286.

(29) Peng, H.; Shen, J.; Edmonds, K. A.; Luebke, J. L.; Hickey, A. K.; Palmer, L. D.; Chang, F.-M. J.; Bruce, K. A.; Kehl-Fie, T. E.; Skaar, E. P.; Giedroc, D. P. Sulfide Homeostasis and Nitroxyl Intersect via Formation of Reactive Sulfur Species in *Staphylococcus aureus*. *mSphere* **2017**, *2* (3), No. e00082–00017.

(30) Shen, J.; Walsh, B. J. C.; Flores-Mireles, A. L.; Peng, H.; Zhang, Y.; Zhang, Y.; Trinidad, J. C.; Hultgren, S. J.; Giedroc, D. P. Hydrogen Sulfide Sensing through Reactive Sulfur Species (RSS) and Nitroxyl (HNO) in *Enterococcus faecalis*. *ACS Chem. Biol.* **2018**, *13* (6), 1610–1620.

(31) Eberhardt, M.; Dux, M.; Namer, B.; Miljkovic, J.; Cordasic, N.; Will, C.; Kichko, T. I.; de la Roche, J.; Fischer, M.; Suárez, S. A.; Bikiel, D.; Dorsch, K.; Leffler, A.; Babes, A.; Lampert, A.; Lennerz, J. K.; Jacobi, J.; Martí, M. A.; Doctorovich, F.; Högestätt, E. D.; Zygmunt, P. M.; Ivanovic-Burmazovic, I.; Messlinger, K.; Reeh, P.; Filipovic, M. R. H2S and NO Cooperatively Regulate Vascular Tone by Activating a Neuroendocrine HNO-TRPA1-CGRP Signalling Pathway. *Nat. Commun.* **2014**, *5* (1), 4381.

(32) Capdevila, D. A.; Walsh, B. J. C.; Zhang, Y.; Dietrich, C.; Gonzalez-Gutierrez, G.; Giedroc, D. P. Structural Basis for Persulfide-Sensing Specificity in a Transcriptional Regulator. *Nat. Chem. Biol.* **2021**, *17* (1), 65–70.

(33) Miranda, K. M. The Chemistry of Nitroxyl (HNO) and Implications in Biology. *Coord. Chem. Rev.* **2005**, *249*, 433–455.

(34) Shafirovich, V.; Lyman, S. V. Spin-Forbidden Deprotonation of Aqueous Nitroxyl (HNO). *J. Am. Chem. Soc.* **2003**, *125* (21), 6547–6552.

(35) Keceli, G.; Toscano, J. P. Reactivity of Nitroxyl-Derived Sulfinamides. *Biochemistry* **2012**, *51* (20), 4206–4216.

(36) Johnson, G. M.; Chozinski, T. J.; Gallagher, E. S.; Aspinwall, C. A.; Miranda, K. M. Glutathione Sulfinamide Serves as a Selective, Endogenous Biomarker for Nitroxyl Following Exposure to Therapeutic Levels of Donors. *Free Radical Biol. Med.* **2014**, *76*, 299–307.

(37) Donzelli, S.; Espey, M. G.; Thomas, D. D.; Mancardi, D.; Tocchetti, C. G.; Ridnour, L. A.; Paolocci, N.; King, S. B.; Miranda, K.

M.; Lazzarino, G.; Fukuto, J. M.; Wink, D. A. Discriminating Formation of HNO from Other Reactive Nitrogen Oxide Species. *Free Radical Biol. Med.* **2006**, *40* (6), 1056–1066.

(38) Sharma, S. V.; Jothivasan, V. K.; Newton, G. L.; Upton, H.; Wakabayashi, J. I.; Kane, M. G.; Roberts, A. A.; Rawat, M.; La Clair, J. J.; Hamilton, C. J. Chemical and Chemoenzymatic Syntheses of Bacillithiol: A Unique Low-Molecular-Weight Thiol amongst Low G + C Gram-Positive Bacteria. *Angew. Chem., Int. Ed.* **2011**, *50* (31), 7101–7104.

(39) Miranda, K. M.; Dutton, A. S.; Ridnour, L. A.; Foreman, C. A.; Ford, E.; Paolocci, N.; Katori, T.; Tocchetti, C. G.; Mancardi, D.; Thomas, D. D.; Espey, M. G.; Houk, K. N.; Fukuto, J. M.; Wink, D. A. Mechanism of Aerobic Decomposition of Angeli's Salt (Sodium Trioxodinitrate) at Physiological PH. *J. Am. Chem. Soc.* **2005**, *127* (2), 722–731.

(40) Huges, M. N.; Wimbleton, P. E. The Chemistry of Trioxodinitrates. Part I. Decomposition of Sodium Trioxodinitrate (Angeli's Salt) in Aqueous Solution. *J. Chem. Soc., Dalton Trans.* **1976**, No. 8, 703–707.

(41) Dickerhof, N.; Paton, L.; Kettle, A. J. Oxidation of Bacillithiol by Myeloperoxidase-Derived Oxidants. *Free Radical Biol. Med.* **2020**, *158*, 74–83.

(42) DuMond, J. F.; King, S. B. The Chemistry of Nitroxyl-Releasing Compounds. *Antioxid. Redox Signaling* **2011**, *14* (9), 1637–1648.

(43) Hrabie, J. A.; Keefer, L. K. Chemistry of the Nitric Oxide-Releasing Diazeniumdiolate ("Nitrosohydroxylamine") Functional Group and Its Oxygen-Substituted Derivatives. *Chem. Rev.* **2002**, *102* (4), 1135–1154.

(44) Shoeman, D. W.; Shirota, F. N.; DeMaster, E. G.; Nagasawa, H. T. Reaction of Nitroxyl, an Aldehyde Dehydrogenase Inhibitor, with N-Acetyl-L-Cysteine. *Alcohol* **2000**, *20* (1), 55–59.

(45) Keceli, G.; Moore, C. D.; Labonte, J. W.; Toscano, J. P. NMR Detection and Study of Hydrolysis of HNO-Derived Sulfonamides. *Biochemistry* **2013**, *52* (42), 7387–7396.

(46) Wong, P. S.-Y.; Hyun, J.; Fukuto, J. M.; Shirota, F. N.; DeMaster, E. G.; Shoeman, D. W.; Nagasawa, H. T. Reaction between S-Nitrosothiols and Thiols: Generation of Nitroxyl (HNO) and Subsequent Chemistry. *Biochemistry* **1998**, *37* (16), 5362–5371.

(47) Johnson, G. M.; Chozinski, T. J.; Salmon, D. J.; Moghaddam, A. D.; Chen, H. C.; Miranda, K. M. Quantitative Detection of Nitroxyl Upon Trapping with Glutathione and Labeling with a Specific Fluorogenic Reagent. *Free Radical Biol. Med.* **2013**, *63*, 476–484.

(48) Sivaramakrishnan, S.; Keerthi, K.; Gates, K. S. A Chemical Model for Redox Regulation of Protein Tyrosine Phosphatase 1B (PTP1B) Activity. *J. Am. Chem. Soc.* **2005**, *127* (31), 10830–10831.

(49) Shen, B.; English, A. M. Mass Spectrometric Analysis of Nitroxyl-Mediated Protein Modification: Comparison of Products Formed with Free and Protein-Based Cysteines. *Biochemistry* **2005**, *44* (42), 14030–14044.

(50) Holden, J. K.; Li, H.; Jing, Q.; Kang, S.; Richo, J.; Silverman, R. B.; Poulos, T. L. Structural and Biological Studies on Bacterial Nitric Oxide Synthase Inhibitors. *Proc. Natl. Acad. Sci. U.S.A.* **2013**, *110* (45), 18127–18131.

(51) Gaballa, A.; Newton, G. L.; Antelmann, H.; Parsonage, D.; Upton, H.; Rawat, M.; Claiborne, A.; Fahey, R. C.; Helmann, J. D. Biosynthesis and Functions of Bacillithiol, a Major Low-Molecular-Weight Thiol in Bacilli. *Proc. Natl. Acad. Sci. U.S.A.* **2010**, *107* (14), 6482–6486.

(52) Newton, G. L.; Dorian, R.; Fahey, R. C. Analysis of Biological Thiols: Derivatization with Monobromobimane and Separation by Reverse-Phase High-Performance Liquid Chromatography. *Anal. Biochem.* **1981**, *114* (2), 383–387.